

## ENTRY FLOW IN A STRAIGHT CIRCULAR PIPE

P. C. SINHA<sup>1</sup> and MEENA AGGARWAL<sup>2</sup>

(Received 28 October 1980; revised 30 June 1981)

### Abstract

Here we discuss the development of the laminar flow of a viscous incompressible fluid from the entry to the fully developed situation in a straight circular pipe. Uniform entry conditions are considered and the analysis is based on the method of matched asymptotic expansions.

### 1. Introduction

In a recent study Singh [5] has discussed the entry flow in a curved pipe. However, his solution is only valid in a region close to the entry. Here we take up the corresponding study for a straight tube and examine the flow development from the entry to the fully developed stage. Various techniques are available in the literature for determining the entry flow in a pipe or channel [1–8]. We follow Van Dyke's approach of matched asymptotic expansions [7] and analyse the problem for the case of uniform flow at the entry.

Accordingly, the development of the flow is studied by considering three regions: (1) an inviscid core, (2) the boundary layer, and (3) the downstream region (Figure 1). Near the entry, the results are found to be in good agreement with the numerical solution of Friedmann *et al.* [3]. The solution for the developing flow breaks down for the streamwise distance  $x = O(Re)$ , where  $Re$  is the Reynolds number of the flow, and so we introduce a new streamwise coordinate  $\xi = x/Re$  in terms of which the new problem determining the downstream flow is found to coincide with the problem discussed by Hornbeck [4].

---

<sup>1</sup>Centre for Atmospheric and Fluids Sciences, Indian Institute of Technology, New Delhi - 110016, India

<sup>2</sup>Department of Mathematics, Indian Institute of Technology, New Delhi - 10016, India

© Copyright Australian Mathematical Society 1982

## 2. Formulation of the problem

Consider the steady axisymmetric flow of a viscous incompressible fluid with kinematic viscosity  $\nu$  in a straight circular pipe of radius  $a$ . The governing equations of motion in non-dimensional form are given by

$$u_r + r^{-1}u + w_x = 0, \quad (1)$$

$$uu_r + wu_x = -p_r + Re^{-1}(u_{rr} + u_{xx} + r^{-1}u_r - r^{-2}u), \quad (2)$$

$$uw_r + ww_x = -p_x + Re^{-1}(w_{rr} + w_{xx} + r^{-1}w_r), \quad (3)$$

with the entry conditions

$$u = 0, \quad w = 1 \quad \text{at } x = 0,$$

and the boundary conditions

$$u = 0, \quad w = 0 \quad \text{at } r = 1 \quad \text{for } x > 0, \quad (4)$$

where  $u$  and  $w$  are the radial and axial velocity components respectively and  $Re = a\bar{w}_0/\gamma$ ,  $\bar{w}_0$  being the characteristic velocity at the entry.

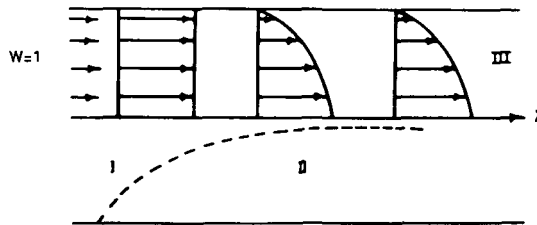


Figure 1. The uniform core model is shown above the centre line. The different regions have been shown below the centre line as follows I: inviscid core, II: boundary layer, III: downstream region.

In the absence of viscosity, the solution in the core is just the undisturbed entry flow given by

$$u = 0, \quad w = 1 \quad \text{and} \quad p = -\frac{1}{2}. \quad (5)$$

## 3. Boundary layer solution

As in the classical boundary layer theory, the effect of viscosity will be confirmed to a thin boundary layer near the wall of the pipe. So, in the boundary layer, we set

$$r = 1 - \beta\eta, \quad u = \beta\bar{u}, \quad w = \bar{w}, \quad p = \bar{p}, \quad (6)$$

where  $\beta = Re^{-1/2}$ . Substituting the expansions

$$\tilde{u} = \tilde{u}_0 + \beta \tilde{u}_1 + \dots,$$

and similar expansions for  $\tilde{w}$  and  $\tilde{p}$  into the equations (1)–(3), the first-order boundary layer equations are obtained as

$$-\tilde{u}_{0,\eta} + \tilde{w}_{0,x} = 0, \quad (7)$$

$$\tilde{p}_{0,\eta} = 0, \quad (8)$$

$$-\tilde{u}_0 \tilde{w}_{0,\eta} + \tilde{w}_0 \tilde{w}_{0,x} = -\tilde{p}_{0,x} + \tilde{w}_{0,\eta\eta}. \quad (9)$$

The boundary conditions are

$$\tilde{u}_0 = \tilde{w}_0 = 0 \quad \text{at } \eta = 0 \quad \text{for } x > 0 \quad (10)$$

and matching with the undisturbed inviscid flow yields

$$\tilde{w}_0 \rightarrow 1 \quad \text{as } \eta \rightarrow \infty, \quad (11)$$

which also holds as  $x \rightarrow 0^+$ . From equation (8) we find that  $\tilde{p}_0 = \tilde{p}_0(x)$ ; but matching requires that  $\lim_{\eta \rightarrow \infty} \tilde{p}_0 = p(\text{core}) = \text{constant}$  for all  $x$  which implies that  $\tilde{p}_0$  is constant. Thus the pressure gradient term will drop out from equation (9). The problem is now reduced to the well known Blasius problem. In terms of the similarity variable  $\zeta = \eta/\sqrt{2x}$  and the Blasius function  $f_0(\zeta)$ , the first-order boundary layer solution is given by

$$\tilde{u}_0 = (2x)^{-1/2}(f_0 - \zeta f_0'), \quad \tilde{w}_0 = f_0'(\zeta). \quad (12)$$

#### 4. Flow due to displacement

The boundary layer thickness grows until it becomes equal to the radius of the pipe. The effect of the growing boundary layer is to accelerate the motion in the core. Since the radial component  $\tilde{u}$  has not been matched yet with the corresponding undisturbed inviscid core velocity, it induces a second-order flow in the core. From (12) it follows that, as  $\zeta \rightarrow \infty$ ,

$$\tilde{u} \equiv \frac{u}{\beta} \sim -\frac{\beta_1}{\sqrt{2x}}, \quad (13)$$

where

$$\beta_1 = \lim_{\zeta \rightarrow \infty} (\zeta - f_0) = 1.21678.$$

This suggests that the flow field in the core will be of the form

$$u = \beta u_1 + O(\beta^2) + \dots, \quad (14)$$

$$w = 1 + \beta w_1 + \dots, \quad (15)$$

$$p = -\frac{1}{2} + \beta p_1 + \dots \quad (16)$$

Substituting the above expansions into the equations (1)–(3) we get the governing equations for the flow due to displacement as

$$u_{1,r} + r^{-1}u_1 + w_{1,x} = 0, \quad (17)$$

$$u_{1,x} = -p_{1,r}, \quad (18)$$

$$w_{1,x} = -p_{1,r}. \quad (19)$$

The appropriate matching condition from (13) is given by

$$u_1 = -\beta_1/\sqrt{2x} \quad \text{at } r = 1, \quad (20)$$

and the entry conditions are

$$p_1 = u_1 = w_1 = 0 \quad \text{at } x = 0. \quad (21)$$

Applying the Fourier sine transform to equation (17) and taking advantage of  $u_{1,x} = \beta_1/(2x)^{3/2} = -p_{1,r}$  at  $r = 1$ , we get the streamwise velocity in the core as

$$w_1 = \frac{\beta_1}{\sqrt{\pi}} \int_0^\infty \frac{I_0(\sigma r) \sin \sigma x}{I_1(\sigma) \sigma^{1/2}} d\sigma. \quad (22)$$

It may be noted that, to leading order, the volume flux deficiency

$$2\pi \int_0^\infty (1 - w) d\eta$$

has an  $x$ -dependence, namely  $\sqrt{x}$ . Thus the corresponding extra total flux in the core associated with  $w_1$ , in (22), must have the same  $x$ -dependence. Also, from equations (18), (19) and (21) we have

$$p_{1,r} = -w_1, \quad (23)$$

and

$$u_1 = -\frac{\beta_1}{\sqrt{\pi}} \int_0^\infty \frac{I_1(\sigma r) \cos \sigma x}{I_1(\sigma) \sigma^{1/2}} d\sigma. \quad (24)$$

Equation (23) implies that there is a fall in the pressure while (22) shows that, correspondingly, the core is being accelerated.

### 5. Downstream expansion

The two-term upstream expansion (15) breaks down when  $\beta w_1 = O(1)$ . The asymptotic behaviour of the integral (22) for large  $x$  is

$$\int_0^\infty \frac{I_0(\sigma r) \sin \sigma x}{\sigma^{1/2} I_1(\sigma)} d\sigma \sim \int_0^\infty \frac{\sin \sigma x}{\sigma^{3/2}} d\sigma = O(x^{1/2}). \quad (25)$$

Hence, it follows that

$$\begin{aligned} \beta w_1 &\sim \beta x^{1/2} \quad \text{for } x \gg 1, \\ \text{that is, } \beta w_1 &= O(1) \quad \text{where } x = O(Re). \end{aligned}$$

This non-uniformity for large  $x$  suggests a contracted downstream variable  $\xi = x/Re$ , and thereby we seek a downstream expansion to complement the upstream expansion in its region of invalidity (Region III, Figure 1). Substituting

$$x = \xi \beta^{-2}, \quad u = -r^{-1} \psi_\xi \beta^2, \quad w = r^{-1} \psi_r, \quad (26)$$

into the equations (1)–(5) we get the first order governing equations, the boundary condition and the matching condition for the downstream expansion as

$$\left[ \frac{1}{r} \psi_\xi \left( -\frac{1}{r} \psi_r \right)_r + \frac{1}{r} \psi_r \left( \frac{1}{r} \psi_{\xi r} \right)_r \right]_r = \left[ \left( \frac{1}{r} \psi_r \right)_{rr} + \frac{1}{r} \left( \frac{1}{r} \psi_r \right)_r \right]_r. \quad (27)$$

$$\psi_\xi(\xi, 1) = \psi_r(\xi, 1) = 0, \quad (28)$$

and

$$\psi_r(0, r) = r. \quad (29)$$

Hornbeck [4] has obtained the finite-difference solution of equation (27) satisfying (28) and (29). Far downstream from the entrance, this flow approaches the Poiseuille parabolic distribution.

### 6. Results and discussion

Figures 2 and 3 represent our two-term upstream solution, one-term downstream solution (Hornbeck) *vis-a-vis* the numerical solution of full Navier-Stokes equations obtained by Friedmann *et al.* [3] at the centreline for  $Re = 100$  and  $250$  respectively. It is seen that the velocity increases more rapidly during the initial development of the flow in comparison to the downstream flow. The figures also indicate that our upstream solution is close to Friedmann's numerical solution near the entry. However, with increasing streamwise distance, our upstream solution deviates from Friedmann's solution which is understandable because the latter does not take into account the displacement effect of the boundary layer

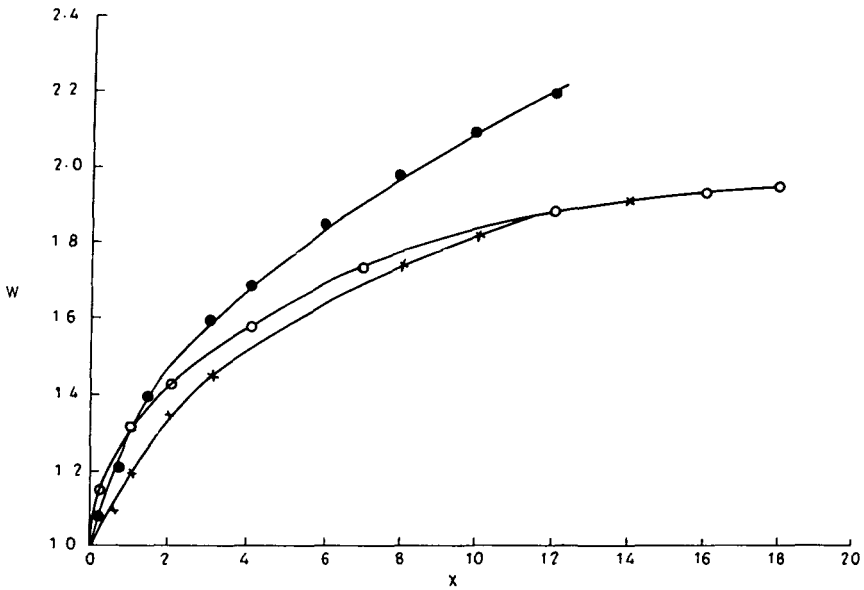


Figure 2. The velocity along the centreline for uniform entry at  $Re = 100$ .

- x—x— full Navier-Stokes solution (Friedmann *et al.*),
- o—o— our one-term downstream solution (Hornbeck),
- our two-term upstream solution.

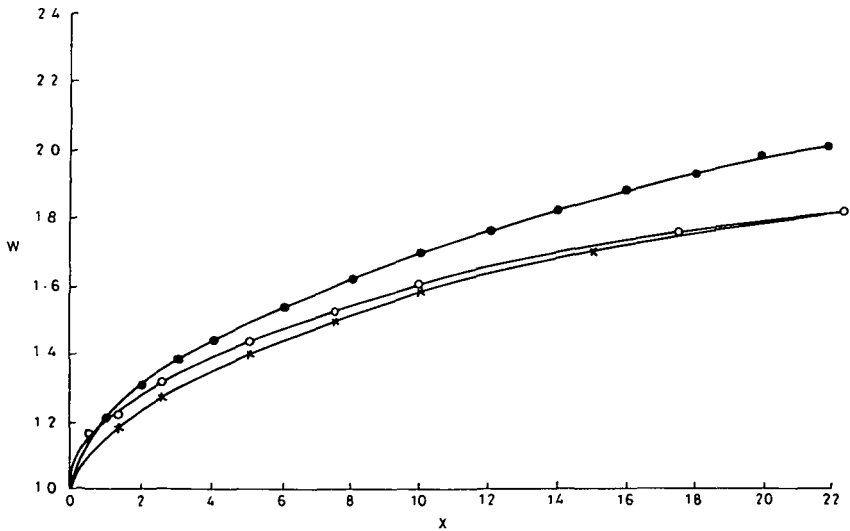


Figure 3. The velocity along the centreline for uniform entry at  $Re = 250$ .

- x—x— full Navier-Stokes solution (Friedmann *et al.*),
- o—o— our one-term downstream solution (Hornbeck),
- our two-term upstream solution.

(see also [2]). The one-term downstream solution (Hornbeck) understandably merges with Friedmann's solution as  $x$  increases.

Figure 4 shows the pressure variation at the centreline for  $Re = 100$  and  $250$  respectively. They show how the upstream and downstream solutions merge in the overlapping region (where  $x \approx 0.15 Re$ ). It is shown that during the initial stages of the development of the flow, the rate of increase in streamwise velocity is larger and consequently the pressure drop is larger in comparison with their values further downstream. This is because the retarded fluid particles in the boundary layer are pushed towards the core more rapidly near the entry where the boundary layer is thinner as compared to the downstream region. The tabulated values of the velocity profile given by Hornbeck have been plotted in Figure 5 for  $Re = 100$ , showing how the fully developed profile is attained.

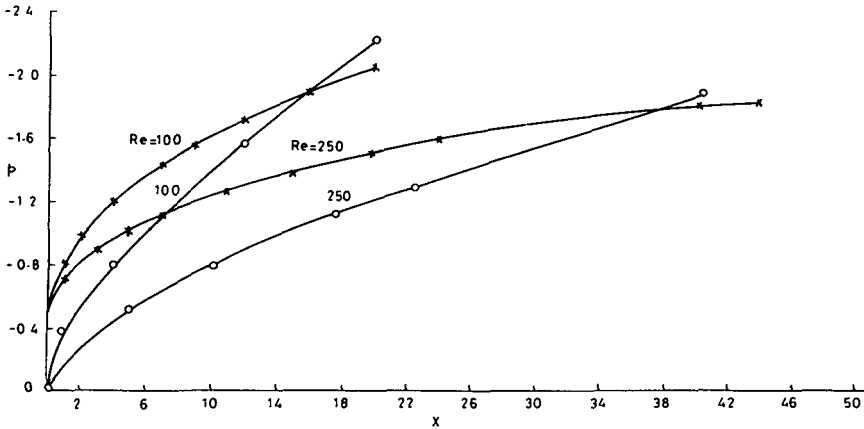


Figure 4. Pressure variation along the centreline.  
—x—x— upstream variation,  
—o—o— downstream variation.

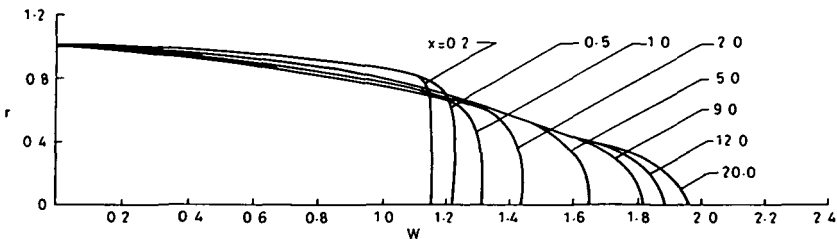


Figure 5. Downstream velocity profile as a function of  $r$  for various values of  $x$  at  $Re = 100$ .

### Acknowledgements

We wish to express our gratitude to Professor M. P. Singh for his help throughout the preparation of this paper. We are also thankful to the referees for making some very useful comments.

### References

- [1] M. Collins and W. R. Schowalter, "Behavior of non-Newtonian fluids in the entry region of a pipe", *Amer. Inst. Chem. Eng. J.* 9 (1963), 804–809.
- [2] D. Fergie and B. W. Martin, "Developing laminar flow in a pipe of circular cross-section", *Proc. Roy. Soc. A* 321 (1971), 461–476.
- [3] M. Friedmann, J. Gillis and N. Liron, "Laminar flow in a pipe at low and moderate Reynolds numbers", *Appl. Sci. Res.* 19 (1968), 426–438.
- [4] R. W. Hornbeck, "Laminar flow in the entrance region of a pipe", *Appl. Sci. Res.* A13 (1964), 224–240.
- [5] M. P. Singh, "Entry flow in a curved pipe", *J. Fluid Mech.* 65 (1974), 517–539.
- [6] E. M. Sparrow, S. H. Lin and T. S. Lundgren, "Flow development in the hydrodynamic entrance region of tubes and ducts", *Phys. Fluids* 7 (1964), 338–347.
- [7] M. D. Van Dyke, "Entry flow in a channel", *J. Fluid Mech.* 44 (1970), 813–823.
- [8] S. D. R. Wilson, "Entry flow in a channel. Part 2", *J. Fluid Mech.* 46 (1971), 787–799.